

Influence of Plasma Discharge Power on the Electrical and Optical Properties of Aluminum Doped Zinc Oxide Thin Films

Yeon-Keon Moon and Jong-Wan Park[†]

Department of Materials Science and Engineering, Hanyang University, 17 Haengdang-dong,
Seongdong-gu, Seoul, 133-791, Korea

(2006년 3월 13일 받음, 2006년 5월 26일 최종수정본 받음)

Abstract Al-doped ZnO (AZO) thin films were grown on type of glass#1737 substrates by DC magnetron sputtering. The structural, electrical and optical properties of the films were investigated as a function of various plasma discharge power. The obtained films were polycrystalline with a hexagonal wurtzite structure and preferentially oriented in the (002) crystallographic direction. The lowest resistivity was $6.0 \times 10^{-4} \Omega\text{cm}$ with the carrier concentration of $2.69 \times 10^{20} \text{ cm}^{-3}$ and Hall mobility of $20.43 \text{ cm}^2/\text{Vs}$. The average transmittance in the visible range was above 90%.

Key words transparent electrode, zinc oxide, DC magnetron sputtering, aluminum doping.

1. Introduction

Transparent conductive oxides (TCOs) have been widely used in optoelectronic devices because of their low electrical resistivity and high transmittance in the visible spectrum region. The most commonly used TCO material for high-quality applications is indium-tin-oxide (ITO). In recent years, however, zinc oxides doped with group III atoms have been attracting much attention as an alternative candidate for ITO due to their inexpensive, abundance, and non-toxic features.¹⁾ Zinc oxide is a II-VI semiconductor with wide direct band-gap of 3.37 eV at room temperature and wurtzite structure. In particular, ZnO film doped with Al, an n-type dopant, has attracted attention as TCO because of its low resistance and high transparency to visible lights. ZnO compounds are of much practical interest for use as optically transparent conducting layers in flat panel displays,¹⁾ organic light-emitting diodes,²⁾ solar cells,³⁾ ultra-violet laser devices,⁴⁾ integrated optics,⁵⁾ piezoelectronic,⁵⁾ gas sensor⁶⁾ and surface acoustic wave (SAW) devices.⁷⁾

The good quality ZnO films have been prepared by many methods, such as sputtering,⁷⁾ reactive thermal and electron-beam evaporation,^{8,9)} pulse laser deposition,¹⁰⁾ chemical vapor deposition,¹¹⁾ spray pyrolysis¹²⁾ and molecular beam epitaxy.¹²⁾ Among the methods, sputtering technique has been widely used to deposit thin films of a broad range of materials because of its advantageous features as simple apparatus,

low deposition temperature and good adhesion and higher density than other methods.

In this paper, we showed the effect of plasma discharge power on the structural, electrical, and optical properties of AZO thin films deposited on type of glass#1737 substrates. The AZO thin films showed good electrical properties as the lowest resistivity of $6.0 \times 10^{-4} \Omega\text{cm}$ and good optical properties as transmittance of above 90% in the visible region.

2. Experimental

AZO thin films on type of glass#1737 (thickness: 0.7 mm) have been prepared using a conventional DC magnetron sputtering system. The target used in this study was sintered from the mixed powder of ZnO and Al_2O_3 , the content of Al_2O_3 in the sputtering target was 2 wt%. The glass substrate was cleaned in acetone, methanol and rinsed in de-ionized water using ultrasonic bath for 10 min, and then dried by the nitrogen gas. The sputtering was performed in only Ar atmosphere with a target-to- substrate distance of 40 mm. An oil diffusion pump with a rotary pump was used to achieve 2.0×10^{-6} Torr before introducing Ar gas. The substrate temperature was measured by a thermocouple gauge and a hot cathode gauge. The substrate temperature was controlled by a feed back controlled heater. The variation in substrate temperature during deposition process was maintained within $\pm 5^\circ\text{C}$. AZO thin films were deposited with various plasma discharge powers ranging from 20 to 80 W. Thick-

[†]E-Mail : jwpark@hanyang.ac.kr

ness of all thin films were fixed 100 nm and deposited for 2-10 min, relatively.

The structural, electrical, and optical properties of AZO thin films were characterized by various techniques. The film thickness was measured using a surface profiler (Alpha-Step 500, TENCOR, USA) and field emission scanning electron microscope (FE-SEM, S-4300, Hitachi). High resolution X-ray diffraction (HRXRD, Bruker D8 DISCOVER, Germany) was used to investigate the crystallinity and crystal orientation of films. The surface morphologies and the surface roughness of the AZO thin films were examined by atomic force microscopy (AFM, AP0190, Auto-Probe CP Multitask Microscopy). The electrical resistivity and Hall mobility were measured at room temperature by the Van der Pauw method. The optical transmittance was measured in visible range by UV-Visible-near-IR spectrophotometer (UV-VIS-NIR spectrometer, Japan Shimadzu UV-3101PC). The elemental compositions of AZO thin films were investigated by Rutherford Back Scattering (RBS, NEC 53DH-2) and Secondary Ion Mass Spectroscopy (SIMS, PH17200 TOF-SIMS)

3. Results and Discussion

3.1 Crystallinity properties

Effects of plasma discharge power on the microstructure of AZO thin films were investigated through the XRD analysis method. The X-ray diffraction patterns of AZO thin films are shown in Fig. 1. As plasma discharge power is increased, the peak intensity is improved. At plasma discharge power of 40 W, the peak intensity is the largest. But the plasma discharge power is increasing over the 40 W, the peak is begun to decrease. The full width at half maximum (FWHM) and grain size of the AZO films using the Scherrer's formula are shown in Fig. 2. Grain size was in reverse proportional to FWHM and grain size was the largest ~27 nm at 40 W. This result is caused by optimized energy supply for growth of thin films. At plasma discharge power of 40 W, increased incident Ar ions energy to the target and increased the sputter yield from target and therefore promoted the growth of thin films. However, sputtered ions could not move in stable lattice location on substrate during the deposition by excessive supply of energy above 40 W. Therefore, the crystallinity is inferior to the AZO thin films deposited below 40 W. This result is a thread of connection between crystallinity and deposition

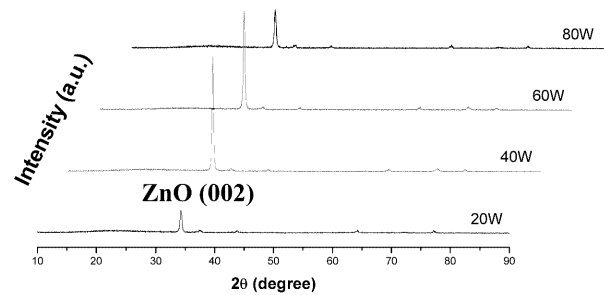


Fig. 1. X-ray diffraction patterns of AZO films deposited with various plasma discharge power.

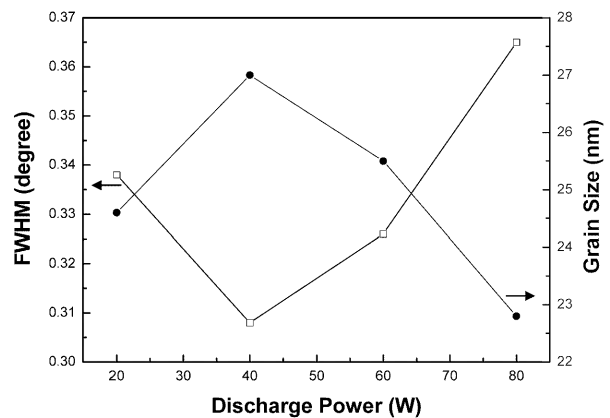


Fig. 2. Full width at half maximum (FWHM) of XRD (002) peaks and the grain sizes for AZO films deposited with various plasma discharge power.

Table 1. Deposition rate with various plasma discharge power

Plasma Discharge Power	Deposition Rate (nm/s)
20 W	0.17
40 W	0.34
60 W	0.54
80 W	0.76

rate (Table 1).

3.2 Electrical properties

Fig. 3 shows dependence of the electrical properties of the AZO thin films deposited with various plasma discharge powers. The resistivity of AZO thin films are decreased with increase of plasma discharge power in the range from 20 to 40 W. The lowest resistivity of $6.0 \times 10^{-4} \Omega \text{cm}$ is obtained at 40 W. A further increase in plasma discharge power had caused increase of resistivity. The resistivity was attributed to relation of carrier concentration (n) and Hall mobility (μ). When the plasma discharge power increased from 20 to 40 W, both carrier concentration and Hall mobility were

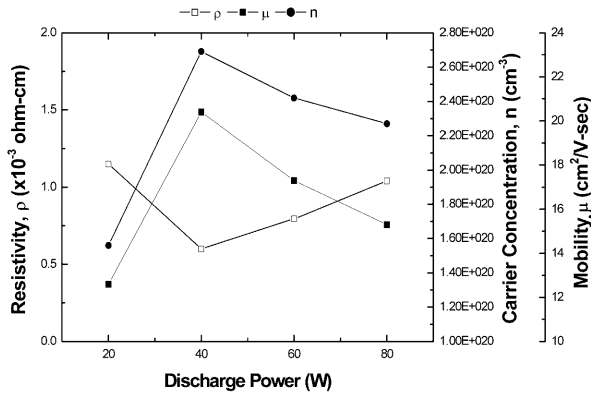


Fig. 3. The surface roughness of AZO films prepared in discharge power, measured by AFM; (a) 20W, (b) 40W, (c) 60W, (d) 80 W.

increased. The maximum values of carrier concentration of $2.7 \times 10^{20} \text{ cm}^{-3}$ and the Hall mobility of $20.4 \text{ cm}^2/\text{Vs}$ obtained at 40 W. At this time, the resistivity obtained a minimal value. However, as plasma discharge power increases further, an opposite variation tendency occurred for the carrier concentration and Hall mobility.

3.3 Optical properties

The transmittance spectra in visible range for AZO films deposited at various plasma discharge power is shown in Fig. 4. All the films exhibited average transmittance of above 90% in the visible region. Fig. 5 shows plots of $(\alpha h\nu)^2$ vs. $h\nu$ for AZO films. The absorption edge for direct interband transition is given the following equation (1) by N. Serpone, D. Lawless and R. Khairutdinov¹³⁾

$$\alpha h\nu = C(h\nu - E_g)^{1/2} \quad (1)$$

, where α denotes absorption coefficient, $h\nu$ denotes photon energy, C denotes constant for a direct transition and E_g denotes optical energy band gap.

The optical energy band gap E_g can be obtained from the intercept of $(\alpha h\nu)^2$ vs. $h\nu$ for direct allowed transition¹⁴⁾. The optical band gap width of AZO films were estimated to be 3.60, 3.74, 3.67 and 3.69 eV at a plasma discharge power of 20, 40, 60 and 80 W, respectively. The variation of absorption edge was shown through the insert graph in Fig. 4. The absorption edge of the transmittance shifted to the shorter wavelength (blue-shift) region up to the plasma discharge power of 40 W. This variety of absorption edge leads to considerable change of optical band gap. This result is attributed to Burstein-Moss (BM) effect. The BM band-

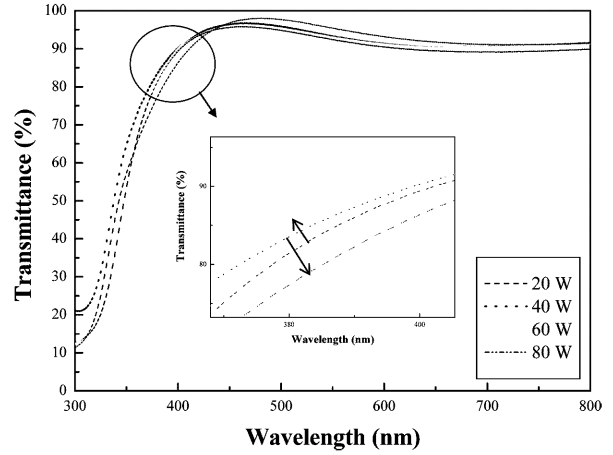


Fig. 4. Electrical resistivity (ρ), carrier concentration (n) and Hall mobility (μ) of AZO films deposited with various plasma discharge power.

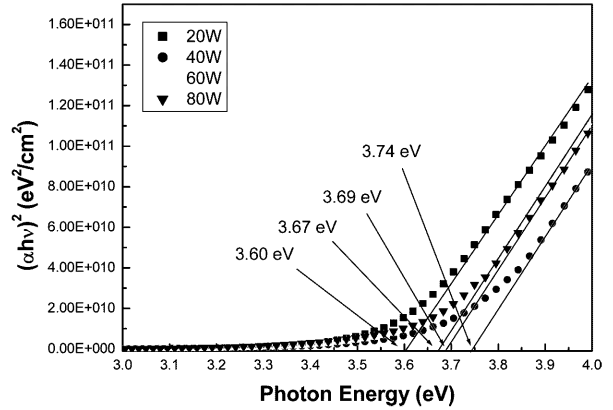


Fig. 5. Optical transmittance spectra of AZO films deposited with various plasma discharge power.

filling effect which shifts positively the band-edge with increasing carrier concentration. This effect is related to the optical band-gap shift. The optical band-gap is described by the following as

$$E_m = E_0 + \Delta E_{BM} - \Delta E_g \quad (2)$$

$$\Delta E_{BM} = \frac{h^2}{8m^*} \left(\frac{3}{\pi}\right)^{\frac{2}{3}} N^{\frac{2}{3}} \quad \Delta E_g = \left(\frac{e}{2\pi\epsilon_0\epsilon_r}\right) \left(\frac{3}{\pi}\right)^{\frac{2}{3}} N^{\frac{2}{3}}$$

, where m^* denotes effective mass ($0.31m_0$), $\epsilon_0\epsilon_r$ denotes dielectric constant of ZnO thin film, E_0 denotes optical band gap of intrinsic ZnO thin film.¹⁵⁾ The measured optical band-gap E_m is the sum of the optical band gap E_0 , plus ΔE_{BM} that due to filling of the conduction band due to donor and minus ΔE_g that due to a change in the nature,

interaction between donors and host crystal and the carrier scattering by ionized impurities.

From the above equations, we are known that the optical band-gap is in proportion to the carrier concentration. The optical band gap was expanded in the range of 20-40 W. These facts are correspond with the above mentioned theory.

3.4 Structure and surface morphology

Fig. 6 shows the root mean square (RMS) roughness value of AZO films deposited with various plasma discharge power. The RMS roughness values were 0.19, 0.59, 0.66 and 0.78 nm for the films deposited with the plasma discharge power of 20, 40, 60 and 80 W, respectively. This indicates that the surface morphology was became rough with increase plasma discharge power. Increase in surface roughness of the films promotes oxygen absorption on the surface of the crystallites to form dangling bonds which the act as electron traps. These electron traps are responsible for the decrease in carrier concentration and Hall mobility. Besides, the rough surface morphology plays a scattering site role in the incident light reducing optical efficiencies.

However, the variety of surface morphology with increasing plasma discharge power seemed to be rather small. Therefore, electronic and optical properties of AZO films would not be affected by the surface roughness in the present case.

Composition of AZO thin films were determined using SIMS referenced by RBS, which shown in Fig. 7. The analysis shows that AZO films exhibited homogenous

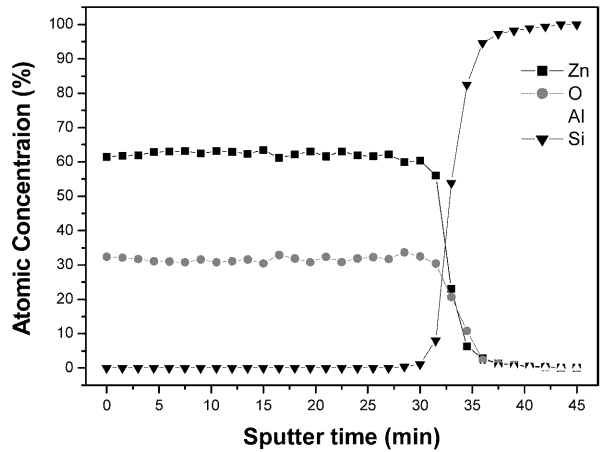


Fig. 7. SIMS depth profiles of AZO thin film deposited at 40 W.

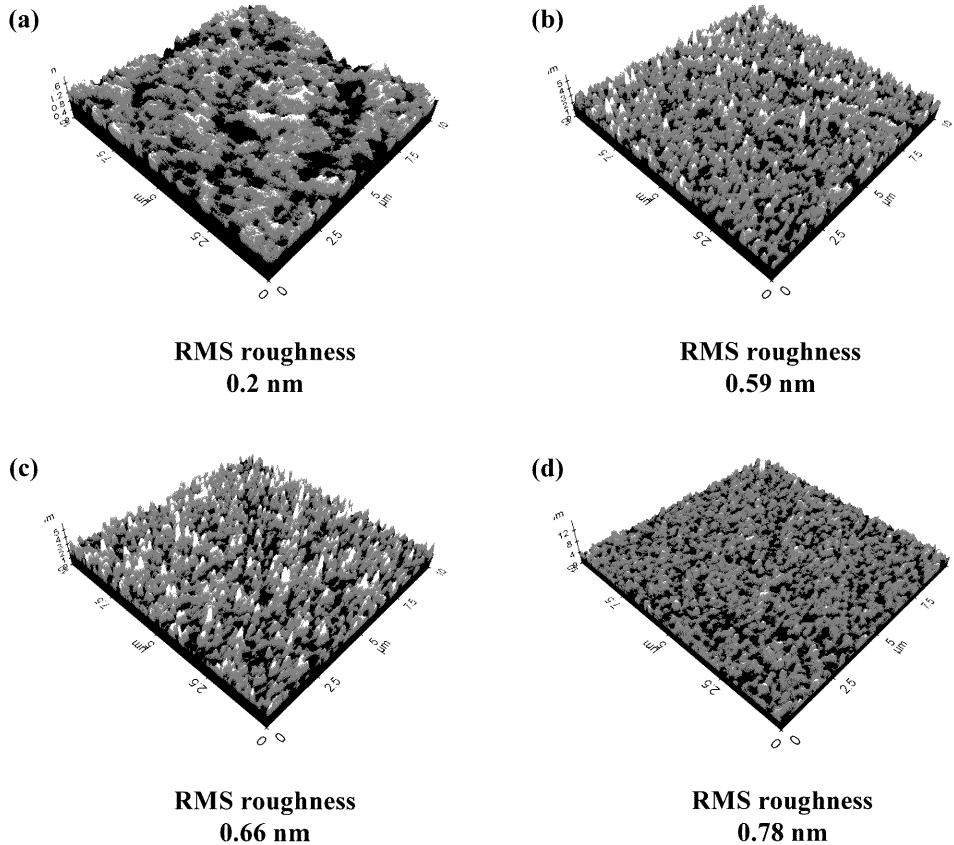


Fig. 6. $(\alpha h\nu)^2-h\nu$ plot properties of AZO films deposited with various plasma discharge power.

composition but the ratio of Zn/O was in general greater than 1. This showed non-stoichiometric chemical states of ZnO¹⁶). The depth profile of AZO film obtained atomic ratio of Zn/O/Al with 62.27/31.46/5.93%. The ratio of Al/Zn by weight is therefore 1.1%, which is greater than that in the target (2 wt%). This is perhaps due to sputter yield property of Zn and Al atoms¹⁷).

4. Conclusion

AZO films have been deposited by DC magnetron sputtering using a ZnO target mixed with Al₂O₃ of 2 wt% on type of glass#1737. The structural, electrical, and optical properties of these films were investigated as a function of various plasma discharge powers. The obtained films were polycrystalline with a hexagonal wurtzite structure and preferentially oriented in the (002) crystallographic direction. The lowest resistivity is $6.0 \times 10^{-4} \Omega\text{cm}$ with the carrier concentration of $2.7 \times 10^{20} \text{cm}^{-3}$ and Hall mobility of $20.4 \text{cm}^2/\text{Vs}$. The average transmittance in the visible range was above 90%. From this work, we could expect the possibility of producing TCO films based on ZnO with good electrical and optical properties by optimizing the plasma discharge power.

References

1. A. E. Delahoy and M. Cherny, *Mater. Res. Soc. Symp. Proc.*, **426**, 467 (1996).
2. Junqing Zhao, Shijie Xie, Shenghao Han, Zhiwei Yang, Lina Ye, and Tianlin Yang, *Synthetic Metals*, **114**(3), 251-254 (2000).
3. Natela R. Aghamalyan, Ruben K. Hovsepian and Armen R. Poghosyan *Proc. SPIE Int. Soc. Opt. Eng.*, **161**, 5520 (2004).
4. Z. K. Tang, P. Yu, G. K. L. Wang, M. Kawasaki, A. Ohtomo, H. Koinuma and Y. Segawa. *Solid State Commun.*, **103**(8), 459 (1997).
5. Navina Mehan, Kondepudy Sreenivas and Abhai Mansingh *Proc. SPIE Int. Soc. Opt. Eng.*, **251**, 5415 (2004).
6. Q. H. Li, Y. X. Liang, Q. Wan and T. H. Wang, *Appl. Phys. Lett.*, **85**(24), 5923 (2004).
7. S. J. Pearton, D. P. Norton, K. Ip, Y. W. Heo and T. Steiner, *Progress in Materials Science.*, **50**(3), 293 (2005).
8. D.C Look, G. M. Renlund, R.H. Burgener and J. R. Sizelove. *Appl. Phys. Lett.*, **85**(24), 5269 (2004).
9. Oshihiro Miyata, Satoshi Ida and Tadatsugu Minami. *J. Vac. Sci. Technol., A* **21**(4), 1404 (2003).
10. Alexander I. Khudobenko, Alexander N. Zherikhin, R.T. Williams, J. Wilkinson, K. B. Ucer, G. Xiong and V. V. Voronov. *Proc. SPIE Int. Soc. Opt. Eng.*, **317**, 5121 (2003).
11. Xiang Liu, Xiaohua Wu, Hui Cao and R. P. H. Chang. *J. Appl. Phys.*, **95**(6), 3141 (2004).
12. Agus Setiawan, Zahra Vashaei et al. *J. Appl. Phys.*, **96**(7), 3763 (2004).
13. N. Serpone, D. Lawless and R. Khairutdinow *J. Phys. Chem.*, **99**, 16646 (1995).
14. I. K. El Zawawi, R. A. Abd Alla, *Thin Solid Films*, **339**, 314 (1999).
15. Haisheng San, Bin Li, Boxue Feng, Yuyang He and Chong Chen, *Thin Solid Films*, **483**(1), 245 (2005).
16. K. L. Chopra, S. Major and D. K. Pandya, *Thin Solid Films*, **102**(1), 1 (1983).
17. Milton Ohring, in *Materials Science of Thin Films*, ACADEMIC, second edition, p. 176.